

Preliminary Report on DSN System Performance Under Local Weather Effects

J. M. Urech
Deep Space Station 62

Local effects of precipitation are studied, and a simplified working model is developed. Experimental results obtained by simulation are in good agreement with the model, showing that it could be an important contribution to system degradation. If this is confirmed, some suggestions for improvement are presented. Nevertheless, definite results with actual rain are not yet available.

I. Introduction

The effects of the weather on X-band telecommunications system performance have generally been of major concern. At stations having only S-band capability, however, subject effects have proven to be very minor for normal tracking. Nevertheless, during DSS 62 continuous support of the planetary radio astronomy program (Jupiter Patrol), the weather problem became a major concern as the minor SNT fluctuations presented catastrophic results when measuring Jupiter temperature of approximately 0.5 K. In some cases the observations had to be cancelled because of rain.

As a result of this problem, it was decided to consult the DSN/Flight Project Interface Design Handbook (810-5) and Ref. 2. In both cases, statistical and probabilistic data are presented for the effects (mainly at X-band) of nonprecipitating clouds. Although this information is especially important for long-term planning, the interest of the station was mainly on the total effects, including precipitation. Although the probability of precipitation is small, some radio astronomy passes

at S-band have undoubtedly been spoiled by rain and critical X-band reception has been badly hampered.

In a further search for weather performance data, other available documents were consulted (Refs. 2-4). However, the information obtained presented a set of curves giving the path losses (dB/km) due to rain for different frequencies and rainfall rates. By using these path losses (which do not include direct antenna effects), the equivalent system noise temperature (SNT) increase may be estimated for certain rain assumptions. The estimates for equivalent SNT increases are normally lower than the values encountered in actual rainfalls.

The extra SNT during rain (not totally explained by cloud attenuation and path losses) as well as the fact that zenith SNT is exceptionally high once rain has subsided has led to the belief that there exists another important contribution related directly to rain falling on the antenna (Mylar and/or reflector). As this potential effect was not contemplated in the consulted documents (Refs. 2-4), a simple experiment was performed to clarify our assumptions.

With the DSS 62 antenna at zenith, a plastic tray was set in front of the horn in order to measure the S-band SNT as a function of the thickness of the various water layers. The initial result of the experiment was absolutely surprising — a system noise temperature of 180 K was achieved with only about 0.5 mm of water. Because of this unexpected result, the entire system was completely checked out and the experiment repeated. However, the second attempt yielded the same results and produced alternating maximum and minimum SNT values for increasing water thickness. The results were not firmly accepted and doubts existed as to whether they were correct and the validity of their interpretation. Nevertheless, it was encouraging to think that the station was on the right track toward the understanding of the precipitation problem.

II. Simplified Working Model

As a first step to clarify the high SNT contribution, studies were made on the properties of water as a thermal radiation absorber and emitter. This, however, did not help as a water layer would only contribute less than 10 K through simple absorption and emission. A clear explanation would probably require an expert in electromagnetic theory, microwaves and radiation theory. In the absence of the latter, numerous documents were consulted on the above fields in order to shed some light on the problem (Refs. 5–7). Although the effect is still not fully understood, it is believed that our simplified working model may help explain the increase in SNT.

A. Effects of Water on Mylar Covering the Horn

Water, as an imperfect dielectric will partially attenuate the electromagnetic radiation by absorption and consequently (Kirchoff law of radiation) partially emit thermal radiation. The most important fact in our case, however, is that the refraction index is fairly high for S- and X-band, thereby acting as a good reflector. If the horn is considered together with the waveguides, diplexer or polarizer (S- or X-band), etc., all the energy received within the design bandwidth will be absorbed with almost no reflection. Reciprocally, all internally generated energy will be radiated out of the horn with almost no back reflection. This may be equivalent to considering the horn as a special black body cavity radiator emitting thermal radiation at ambient temperature. Transmitted to the outside, the radiation is normally unnoticeable. However, if a water film or other reflective dielectric is present in front of the horn, part of the energy will be reflected back, some absorbed by the film, and the remainder will be transmitted outwards. If r is the fraction of incident power reflected, α is the fraction of incident power absorbed, and t is the fraction of incident power transmitted, then $r + \alpha + t = 1$.

However, the thermal radiation power e emitted by the film (if in local thermodynamic equilibrium) is, according to the Kirchoff law of radiation, identical to the absorbed radiation α . Therefore, if the horn and dielectric film are at ambient temperature T_0 , the power (noise temperature) detected by the receiver for this effect will be:

$$T = T_0 (r + e) = T_0 (r + \alpha) = T_0 (1 - t)$$

which is the same as the well-known formula generally used to determine the noise temperature contribution of any attenuation or mismatch loss.

Obviously any signal received or transmitted will be attenuated by $10 \log t$ (dB's). The power reflection and transmission coefficients for a dielectric film in air are (Ref. 8)

$$r = \frac{\rho^2 [(1 - A^2)^2 + 4A^2 \sin^2 \Phi]}{(1 - A^2 \rho^2)^2 + 4A^2 \rho^2 \sin^2 (\Phi + \chi)}$$

$$t = \frac{A^2 [(1 - \rho^2)^2 + 4\rho^2 \sin^2 \chi]}{(1 - A^2 \rho^2)^2 + 4A^2 \rho^2 \sin^2 (\Phi + \chi)}$$

where

$A = \exp(-2\pi d n/\lambda_0 K)$ amplitude transmission coefficient for single film transversing

$\phi = 2\pi d n/\lambda_0$ phase shift for single film transversing

$\rho = n - 1/n + 1$ amplitude reflection coefficient for a single reflection

$\chi = \tan^{-1}(2nK/n^2 - 1)$ phase shift of single reflection

d = film thickness

n = refraction index

λ_0 = wavelength in air

$K = tg\delta/2$

$tg\delta = \sigma/\omega\epsilon$ loss tangent or dissipation factor

σ = dielectric conductivity

ϵ = dielectric constant

The above expressions have been evaluated for the following cases of general interest:

(Fig. 1) Temperature and attenuation of a water film in S-band

(Fig. 2) Temperature and attenuation of a water film in X-band

(Fig. 3) Temperature and attenuation of snow and ice in S-band

(Fig. 4) Temperature and attenuation of snow and ice in X-band

These results should be considered indicative rather than totally accurate, because the values for the dielectric constant and dissipation factor at S- and X-band have been interpolated from the data presented for other frequencies in Table 4-19 of Ref. 2 (as the only source presently available). Nevertheless, it is considered that this questionable accuracy would not invalidate the following important conclusions:

- (1) A very thin water film on the Mylar will contribute to very high system noise temperatures, especially at X-band. This is mainly due to the high refraction index of water for these frequencies, thereby making it a good reflector, reducing also the effective wavelength ($\lambda = \lambda_0/n$).
- (2) Figures 1 and 2 are evaluated up to very thick water films, not that they can be formed by rain, but in order to permit validation of the model by feasible experiments. In both cases, the puzzling result initially obtained of alternating maximum and minimum SNT is confirmed. This occurs at multiples of $\lambda/4$ (wavelength in water) when the internal reflections of the film are in or out of phase with respect to the main reflection at the interface.
- (3) Figures 3 and 4 clearly show that SNT contributions for freshly fallen snow, hard packed snow, and ice are in any case much smaller than for liquid water. Subject contributions are a consequence of the lower refraction indexes: 1.1, 1.22 and 1.78, respectively, as compared to 8.83 and 6.5 for liquid water at S- and X-band.

B. Effects of Water on Antenna Reflector Surface

This could also be considered another potential contribution to the general degradation during rain. However, it is difficult to confirm experimentally. Therefore, if the model used in the previous case is deemed valid, the reflection losses may be estimated using a similar expression.

The power reflection coefficient for a dielectric film covering a perfect reflector is (Ref. 8), using the same notation as before,

$$r' = \frac{(\rho + A^2)^2 - 4A^2 \sin^2(\phi - \chi/2)}{(1 + \rho A^2)^2 - 4\rho A^2 \sin^2(\phi + \chi/2)}$$

Based on a temperature contribution of $T = T_0 (1 - r')$, the following values were estimated:

Liquid water		
Film thickness, mm	S-band temp, K	X-band temp, K
0.25	2.6	0.81
0.50	2.7	7.4
0.75	4.3	33.0
Snow		
10	0.005	0.42
20	0.11	0.58

As can be seen, this potential contribution will be negligible when compared with similar films on the Mylar, as has been previously shown.

It could be argued that the above models would not be applicable to real cases as a water film may not be formed. This is partially true because the water by surface tension may form dispersed drops instead of a film. Nevertheless, if the horn illumination is supposed to be uniform, and the temperature contribution model practically linear for small thickness, the effect of the dispersed drops could be estimated assuming a film thickness equivalent to the total amount of water on the surface.

III. Empirical Results

Once the simplified working model was developed, a test, similar to the one mentioned in the introduction, was carefully prepared for S-band at DSS 62. A flat plastic tray was fabricated having a slightly larger size than the horn window. With the antenna at zenith, the tray was perfectly leveled in front of the horn and barely touching the Mylar. Then each time a controlled amount of water was added, a measurement of the system noise temperature was taken with the noise adding radiometer. For the first two points obtained (equivalent to film thickness of 0.5 and 1 mm), the film was not actually formed, but the drops were purposely distributed more or less uniformly.

All SNT data points have been directly plotted in Fig. 1, and the solid line curve is the theoretical water film contribution (not the total SNT including waveguide losses, receiver, etc.). The results, in general, are in good agreement with the simplified model, thereby confirming two aspects: First, that the model is valid for the study of these types of effects; second and more important, that the water film on the Mylar may have a catastrophic effect on telecommunications performance.

A similar test setup was prepared for X-band at DSS 63. In this case, due to the geometry of antenna and X-band cone, the horn window could not be set horizontally and therefore not parallel to the levelled tray. This has some implication on the angle of reflection which may slightly jeopardize the test results. However, the SNT measurements, which are plotted in Fig. 2, are also in fairly good agreement with the model. As should be expected and can be seen from Figs. 1 and 2, the water temperature contribution of very thin films is much higher for X-band: 95 K vs 25 K for an equivalent film of one-tenth millimeter.

No similar tests have been conducted to check Figs. 3 and 4 (snow and ice) and therefore they should be taken only as indicative.

IV. Suggestions for Degradation Reduction

The possibility of an equivalent water film forming on the Mylar surface during rain will be directly related to two opposing factors:

- (1) The amount of water impinging on the surface which is a function of the rainfall rate direction and the antenna position.
- (2) The water drainage on the same surface which is also a function of the type of surface and its affinity to water, wind and rain intensity and direction, and antenna position.

Although it is very difficult to quantify all these factors, one technique which will enhance the situation is to improve the water drainage as much as possible. In this regard, many different ideas may be proposed. Some of our suggestions are presented below for further study, testing or development, based mainly on the X-band feed as the case of major concern.

- (1) The capability of Mylar to retain water drops seems to be low but there may exist another material with better performance, or a water repellent coating.

- (2) The ring connecting the Mylar to the X-band horn is quite thick. This could retain some water on the internal edge which may not be negligible when compared to the window size.
- (3) A special type of plastic shield wiper having low refraction index and dissipation factor may be designed and tested.
- (4) A vibrating window (acoustically or ultrasonically activated) might be developed.
- (5) A centrifugal double window similar to the ones used in boats might be used. This method, if feasible, would be absolutely efficient in draining water (see sketch A of Fig. 5).
- (6) A well-designed system of nozzles (jets) blowing compressed air at high-speed over the Mylar window might be employed.

As this system is relatively simple, it has been tentatively tested in a rudimentary form. A standard nozzle attached to a small plastic fixture (see sketch B of Fig. 5) was temporarily mounted near the X-band horn (outside its field of view) and connected by a hose to an air-compressor with a pressure of 90 psi. With a "rain emulator" (a plastic watering-can) a more or less uniform shower was generated over the Mylar, obtaining a system noise temperature of about 180 K. Then with the nozzle blowing the SNT came down to about 100 K. The test was repeated with a lighter shower, changing the SNT from 85 K to 55 K when blowing.

V. Conclusions

From the theoretical and experimental results of this study, the logical conclusion would be to believe that the local rain effect may be of prime importance. However, to reach a firm conclusion, further tests have to be performed during actual rain in order to measure the relative contributions of the path and local effects and determine if they are separable. For a simple qualitative test, the rudimentary system suggested in IV-6 above has been temporarily left installed, but no test data is yet available.

References

1. Greenhall, C. A., "Examination of the DSN X-Band Weather Specifications," in *The Deep Space Network Progress Report 42-45*, pp. 197-208, Jet Propulsion Laboratory, Pasadena, Calif., July 15, 1978.
2. *Reference Data for Radio Engineers*, 5th edition, ITT Handbook.
3. Fink, D. G., *Electronic Engineers' Handbook*, McGraw Hill, New York.
4. Marton, L., and Meeks, M. L., *Methods of Experimental Physics: Volume 12, Astrophysics, Part B: Radio Telescopes*.
5. Ramo, S., Whinnery, J. R., *Fields and Waves in Modern Radio*, 2nd edition, Wiley, 1953.
6. Eisberg, R., and Resnick, R., *Quantum Physics*, Chapter 1, "Thermal Radiation."
7. Menzel, D. H., selected papers on the transfer of radiation.
8. Blevis, B. C., "Losses Due to Rain on Radomes," *IEEE Trans. Ant. Prop.*, pp. 175-176, Jan. 1965.

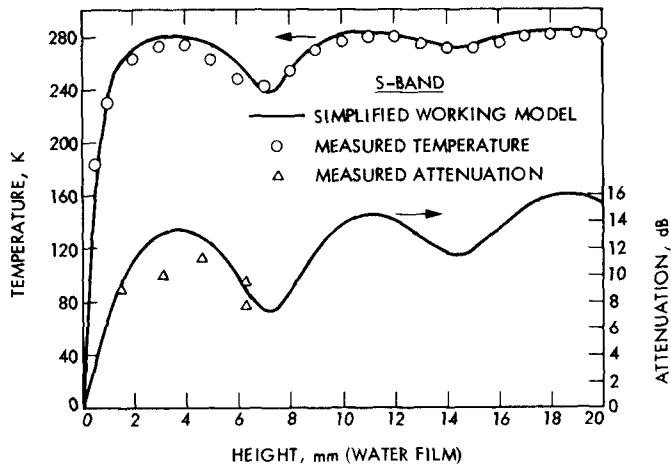


Fig. 1. Temperature and attenuation of a water film in S-band

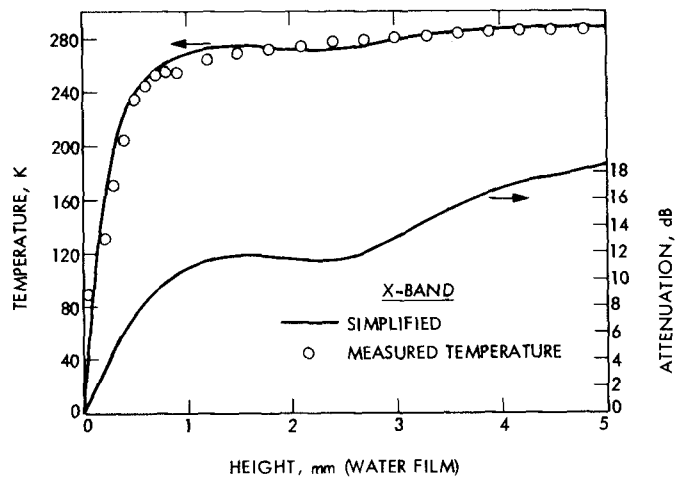


Fig. 2. Temperature and attenuation of a water film in X-band

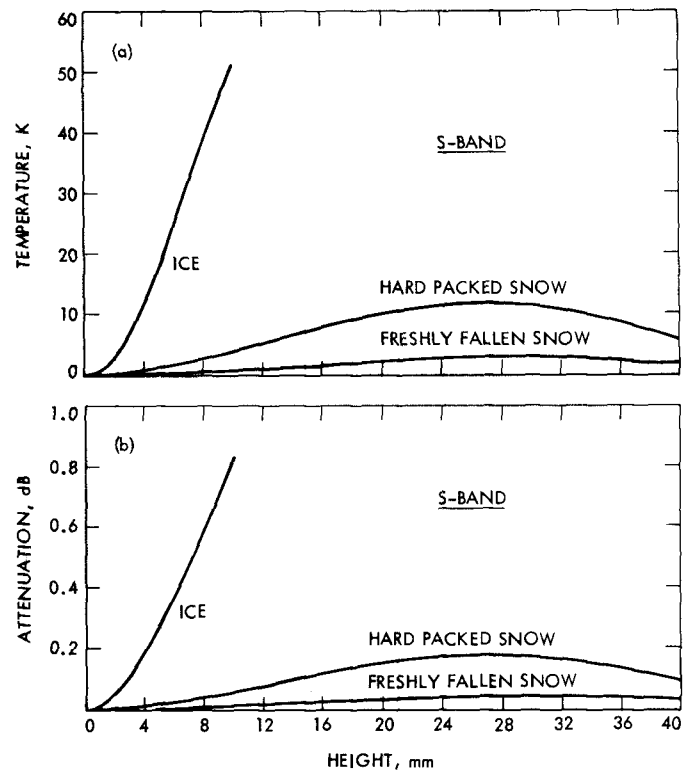


Fig. 3. Temperature and attenuation of snow and ice in S-band

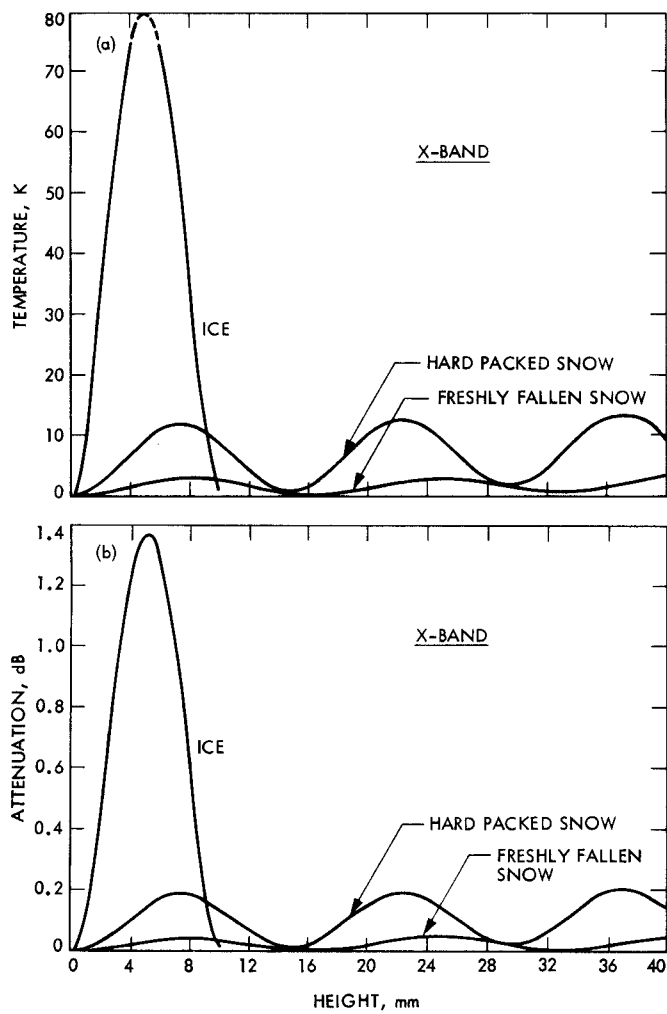
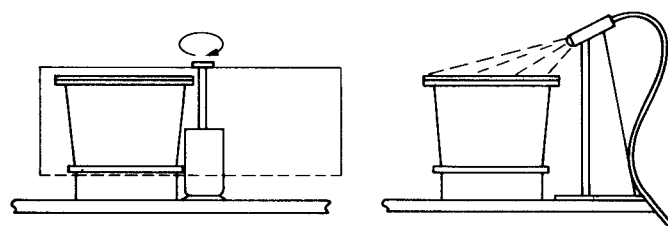


Fig. 4. Temperature and attenuation of snow and ice in X-band



X-BAND HORN, SKETCH A:
CENTRIFUGAL SUGGESTION

X-BAND HORN, SKETCH B:
AIR BLOWING NOZZLE
SUGGESTION

Fig. 5. Proposed test configuration